

Displacement Fields in Footing-Sand Interactions under Cyclic Loading

S. Joseph Antony, Z. K. Jahanger

Abstract—Soils are subjected to cyclic loading in situ in situations such as during earthquakes and in the compaction of pavements. Investigations on the local scale measurement of the displacements of the grain and failure patterns within the soil bed under the cyclic loading conditions are rather limited. In this paper, using the digital particle image velocimetry (DPIV), local scale displacement fields of a dense sand medium interacting with a rigid footing are measured under the plane-strain condition for two commonly used types of cyclic loading, and the quasi-static loading condition for the purposes of comparison. From the displacement measurements of the grains, the failure envelopes of the sand media are also presented. The results show that, the ultimate cyclic bearing capacity (q_{cyc}) occurred corresponding to a relatively higher settlement value when compared with that of under the quasi-static loading. For the sand media under the cyclic loading conditions considered here, the displacement fields in the soil media occurred more widely in the horizontal direction and less deeper along the vertical direction when compared with that of under the quasi-static loading. The 'dead zone' in the sand grains beneath the footing is identified for all types of the loading conditions studied here. These grain-scale characteristics have implications on the resulting bulk bearing capacity of the sand media in footing-sand interaction problems.

Keywords—Cyclic loading, DPIV, settlement, soil-structure interactions, strip footing.

I. INTRODUCTION

SOILS are periodically subjected to cyclic loading in situ in situations such as under earthquakes, machine vibrations and in the construction of foundations, pavements and railways ballast. In foundation engineering, the magnitude of the cyclic loading (q_{cyc}) is generally small, as compared to the quasi-static load (q_s) of the footing; $q_{cyc}/q_s \leq 0.5$. The value of this ratio is usually 0.1-0.3 in many earthquake scenarios, whereas this ratio greater than 0.5 represents an extreme event [1]. Under the cyclic loading, foundations could experience a significant level of settlement that causes structural damage [2]. The design of the foundations under the cyclic loadings (q_{cyc}) is a challenging task for the geotechnical engineers due to lack of information on how failure occurs at local and global scale in soil bed under cyclic loadings.

The term cyclic loading is defined as a system of repeated loads that shows a constancy rate in the amplitude and the

frequency is less than 1.0 Hz [3]. Different types of the environmental cyclic loadings encountered in practice such as due to the waves, wind and earthquakes. Man-made cyclic loading can occur from the traffic construction and blasting operations and when using the rotating machinery [4]. Traffic might generate vibrations of a periodic character and the blasting effects can be detrimental to the foundation of an elevated railway [5]. Many researchers have studied on the effects of the cyclic loading on the failure of the footings interacting with soil using different theoretical and experimental methods. Salem et al. [6] have defined the cyclic loading failure of the footings interacting with the soil as the number of loading cycles required to reach liquefaction (quick condition) or when an axial strain of 5% is reached. Soil liquefaction defines a phenomenon when a saturated or partially saturated soil significantly loses their strength and stiffness in response to the cyclic loading, causing the sand to behave like a liquid. Andersen [7] suggested that the failure load caused by cyclic loading is defined at a permanent shear strain of 15%.

Numerous researchers have studied on the behaviour of the sand bed under the cyclic loads using different materials and techniques [1], [2], [8]-[10]. They reported that excessive soil deformations are produced under cyclic loading and the strains accumulate with increasing the number of cycles, causing damage to building foundations. The cyclic loading could have a significant effect on sandy soil. The strength of the sand under the cyclic loading could be less than that under the quasi static loading with the same level of stress amplitude [9]. Asakereh et al. [11] have studied the cyclic response of footing on geogrid-reinforced sand with a void that modelled a tunnel. They stated that, the rate of settlement of the footing was significantly large during the initial loading cycles; thereafter the rate of settlement decreases significantly as number of the loading cycle increases. However, experimental observations of the local scale kinematic failure mechanisms in silica sands beneath shallow footing under the vertical cyclic loading are scarce in the literature. Therefore, the current study deals with the specific case of the plane strain surface footing interacting with dense sand subjected to different types of cyclic loading. The aim is to understand the failure mechanism and local deformation field in the dense sand under vertical cyclic loadings considered here, and their comparison with the quasi-static loading condition.

II. MATERIAL AND EXPERIMENTAL METHODS

A. Sand Sample and Experimental Setup

The sand used in this study is a relatively uniform silica

S. J. Antony is now with School of Chemical and Process Engineering, University of Leeds, LS2 9JT, Leeds, UK (e-mail: S.J.Antony@leeds.ac.uk).

Z. K. Jahanger is now with Department of Water Resources Eng., College of Engineering, University of Baghdad, Iraq (corresponding author, e-mail zuhairkadhim@gmail.com_and ORCID 0000-0003-2869-9178). Formerly, PhD researcher at University of Leeds, UK.

sand of grain sizes between 0.07 and 0.9 mm that is a disturbed dry sample (kiln dry sand) obtained in UK [12]-[17]. The properties of the sand were characterized according to the American Society for Testing and Materials [18], [19]. Table I shows the particle size distribution properties of the sand and its experimentally measured properties. Based on these data, the soil chosen is classified as poorly graded sand (SP) according to the Unified Soil Classification System [9], [20]-[22].

For conducting the DPIV experiments, a planar model box was designed and constructed to satisfy both the mechanical and optical requirements. The former requirement is that the granular box was able to sustain the external loading while minimising the out of plane deformation of the walls (including the front measuring side of the box) under the ultimate load. The latter requirement pertains to enabling the image recording of the grains at the front face of the box model. The front face of the box was made of 15 mm thick Perspex sheet (rigid). The backside of the box was made of 10 mm thick smooth aluminium sheet, whereas the side of the box was made of aluminium frames having the dimension of 25 mm × 39 mm. The aluminium planar model has an internal dimension of 460 mm×300 mm×39 mm. Hence, the dimensions of the test box were kept much greater than that of the footing to minimize the boundary effects. The relatively rough rigid aluminium footing dimensions were of 38 mm × 38 mm × 15 mm. The experiments presented here have been performed as shown in Fig. 1, wherein the planar box filled with sand is placed stationary, while the footing model was indented in the sand bed.

TABLE I
PHYSICAL PROPERTIES OF THE DENSE SAND

Type of the test	Unit	Results
Dry density, γ_d	kN/m ³	16.2
Void ratio, e_o		0.62
Relative density, D_r	%	76
Peak friction angle, ϕ_{peak}	degree	44.8
Max. dry density, γ_{dmax}	kN/m ³	16.50
Min. dry density, γ_{dmin}	kN/m ³	14.23
Mean grain size, D_{50}	mm	0.37
Uniformity coefficient, C_U		1.55

The ratio of the width of the footing (B) to the mean grain size D_{50} ; i.e., $B/D_{50} \geq 100$, (which is within the permissible limit [15], [16], [21], [23]) to minimise any size effect arising from the relative sizes of the footing and the sand grains. A small gap of 1 mm was set between the rear surface of the footing and the rear side of the aluminium wall to minimise any resisting frictional forces between these surfaces that it was verified that no significant leakage of the grains occurred through this gap during the tests. A high speed camera HSC (Photron Fastcam SA5) was used in front of the planar model placed in an Instron 5 kN loading machine. The HSC with an allowable frame speed up to 100000 frames per second (fps) was used.

B. Preparation of the Dense Sand Packing

The homogeneous packing of dense sand was prepared in five layers using falling pouring technique method based on Kumar and Bhoi [24] and Jahanger et al. [15], [16], at a constant rate, such that the materials formed layers of ~55 mm thick each. The mass of sand grains laid in the box correspond to the required height and the packing density of the sand. Then the sand layer was compacted using 60 blows in 0.035 m lifts per layer by a hand compaction of 1.10 kg weight [15]-[17], [20]. The preparation of the sand test box was done directly on the loading machine baseplate to minimise any disturbing of the sand grains.

C. Cyclic Loading Types and Test Programme

Two types of strain-controlled tests under the quasi-static and the cyclic loading pattern were performed (Fig. 2). Details of the parameters of the model tests are presented in Table II. For studying the mechanical response of the footing-sand interactions, experiments were carried out to measure the quasi-static ultimate bearing capacity (q_{ult}) and the corresponding settlement of the footing (S_u). The quasi-static load was applied on the footing at a slow rate (0.05 mm/s) resolution and up to 10 mm using the Instron machine with 0.1 N resolution.

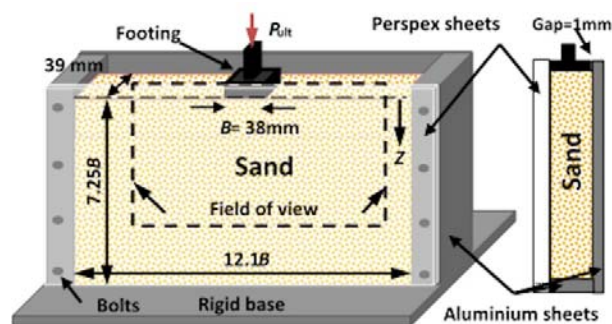


Fig. 1 Experimental setup using DPIV

The macroscopic load-settlement relations of the footing on the dense sand were measured at a frequency of 1 Hz. Though the quasi-static curve is drawn for the time as in the cyclic loading test, in reality the test continuous until the peak load was achieved as shown in Fig. 2 (c). The cyclic load experiments were conducted using the Instron machine for the selected types of the cyclic load to measure the cyclic ultimate bearing capacity (q_{ultcyc}) and the corresponding settlement of the footing (S_{ucyc}). These are defined here to simulate different types of the machines cyclic loads, such as type1 cyclic load selected which the loading history consists of stepwise increasing load cycles (Fig. 2 (a)). Type2 cyclic load was selected based on the cyclic plate loading test (PLT) in which the amplitudes increase with the increase of the cycles [9].

The tests were conducted by first applying the initial static settlement, $S=S_i=2$ mm with corresponding initial static stress $q=q_s$, on the footing (Fig. 2 (a)). Before applying the cyclic settlement (S_{cyc}), the initial static settlement (S_i) was applied [9]. The allowable load of the dense sand bed was first applied

under the initial static settlement of $S_i=2$ mm. Then, the cyclic loadings were applied using a sinusoidal loading. The intensity of the load on the footing was then varied between the $S=S_i$ and $S=S_i + S_{cyc}$ with a frequency of 0.23 Hz and 0.35 Hz (cycle/sec) for cyclic loading type 1-2 respectively (Fig. 2 (a)). The amplitude was incrementally increased at 1mm per each cycle. The cycles of the loading, unloading and reloading were continued until the ultimate load and the subsequent failure of the sand was reached (Fig. 2 (b)).

TABLE II
 DETAILS OF THE LABORATORY MODEL TESTS

Tests	q_s/q_{ult}	q_{ultcyc}/q_{ult}
Quasi-static	-	-
Type 1	0.59	0.155
Type 2	0.59	0.165

D. Digital Particle Image Velocimetry (DPIV) Analysis

DPIV pertains to the digital platform of particle image velocimetry [12]-[17]. PIV is often used in the field of fluid mechanics to track the motion of particles in the fluid flow using the tracer particles [25]. Researchers have used Particle Image Velocimetry (PIV) to study the displacement and (*or*) strain distribution in some cases of granular packing under quasi-static loading conditions [12]-[17], [26]-[28].

The macroscopic load-settlements of the footing on the dense sand were recorded from the tests. In the present study, the DPIV camera lens was focused normal to the plane of the footing structures-soil interface region of ~ 273 mm \times 154 mm and two light sources were used to illuminate the rig (Fig. 1). This was further sub-divided into 129600 interrogation areas (IA) of minimum of 4×4 pixels each covering a zone of about 0.57 mm \times 0.57 mm which contains a minimum of three grains in each IA. The resolution of the images was 1920×1080 pixels. This corresponds to a scale of ~ 0.14 mm per pixel in this study. Hence, the PIV experimental measurements made here are at the local-scale. However, as the loading condition is cyclic in this study and the storage capacity of the acquisition system (60 seconds of recording capacity), the recording at 250 fps was found to be adequate until soil failure was reached. This acquisition of 250 fps of the recorded images was captured having spatial resolution of about 0.028 mm- 0.0001 mm.

In this study, Dynamic Studio Software Platform (DSSP) was used to analyse the digital images acquired during test using DPIV [29]. This functionality built in the DSSP was used to analyse the digital frames of the grains, and to calculate velocity vectors of the grains and their evolution during load application within the sand layer between two successive images [12]-[17], [30]. The mean number of particles per maximum IA should vary between 10 and 25 [29]. The convergence limit equals 0.01 pixel was employed in the image analysis. A typical mean size of sand grain was represented by a patch of 3 pixel \times 3 pixel to reduce PIV error [31]. Each of these patches was tracked using an adaptive PIV method, to identify the deformation field of sand grains between successive images, to a measurement precision of 0.014 mm for the field of view used during these experiments.

This space-pixel dimension of the measurement was calibrated by printing a known scale on the test box along the horizontal and vertical directions. The variation in the image scale in both horizontal and vertical direction was not significantly different. Furthermore, texture enhancement of the sand with coloured grains was adopted to increase the accuracy of the image correlation. The tests were repeated at least twice to verify the repeatability and the consistency of the test data [12]-[16], [24]. The displacement measures, i.e. horizontal displacement (S_h), vertical displacement (S_v), and the resultant displacement (S_R) were calculated under a given load in total.

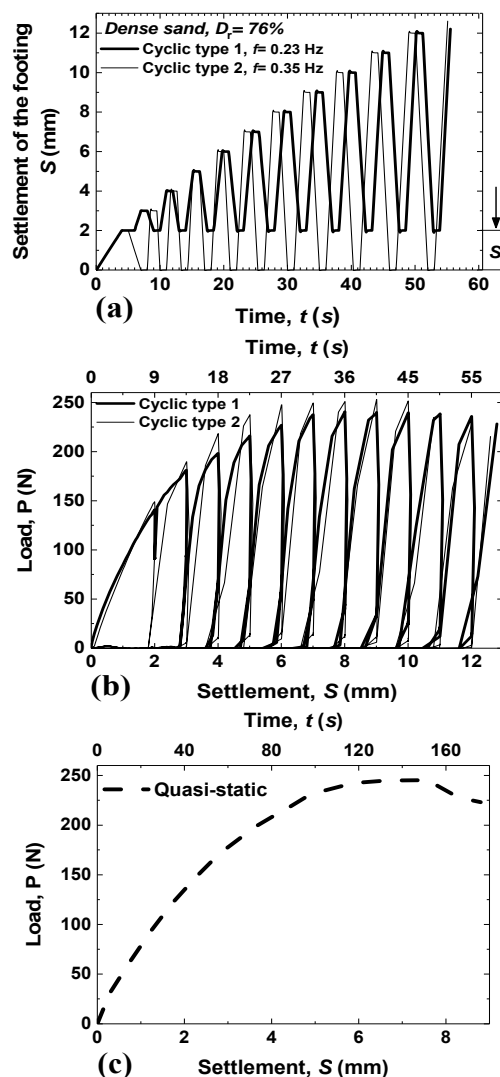


Fig. 2 Pattern of cyclic and quasi-static loadings

E. Scale Effects and Limitations

It is acknowledged that the scale effects of the footing model could affect the estimations of their strength characteristics [15]. Though the small-scale models are widely used to investigate the behavior of the full scale foundation, there could be some differences between the results of the experiments using laboratory models and the prototype [32], [33]. To minimize the scaling effect, it was suggested that the packing density of the tested sample should not pertain too

close to its maximum void ratio (e_{max}) and minimum void ratio (e_{min}) [34]. These suggestions were accounted for in the current study to minimise the scale effects.

The authors wish to point out that, in the case of strip footings used in practice, 3D condition could exist around the ends of the strip footings even if the footing is long. However, for most parts of long strip footings, plane strain condition could exist [15], [16], [35], [27] as assumed in the current 2D plane strain experiments [15], [16], [36].

III. RESULTS AND DISCUSSION

We observed that (Fig. 2 (b)) the ultimate cyclic bearing capacity (q_{ultcyc}) occurred at higher settlement value compared to the quasi-static experiment conducted here. This agrees with the previous quasi-static and cyclic loading results of sand [9], [37]. In general, a well-defined peak was obtained for the cases of the cyclic loading tests and the failure corresponds to general shear failure [38]. Mostly, a peak value of the cyclic load response was obtained within the first seven cycles of loading. The ratio of ultimate vertical cyclic settlement (S_{ucyc}) under the ultimate cyclic load to B , i.e., S_{ucyc}/B is $\sim 13-18\%$ in all cases of the cyclic loading considered in the study. This ratio is about 11.8% in the case of quasi-static loading test (Fig. 2 (c)). These measures are consistent with the results reported earlier for example, Andersen [7]. The slight increase of this ratio in the case of cyclic loading experiments can be due to the potential increase in the soil stiffness as sand accommodates relatively large strain in the soil beneath the footing under the ultimate load [9] (Figs. 2 (b) and (c)).

IV. LOCAL DISPLACEMENTS OBTAINED FROM THE DPIV ANALYSIS

Fig. 3 compares the DPIV based measures of the mean resultant displacement vector under the ultimate load. In this, scalars contours of the vertical (Fig. 3 (i)) and horizontal (Fig. 3 (ii)) displacements are also superimposed for the comparison purposes. This visualization illustrates whether horizontal or vertical soil displacements dominate the failure mechanism mobilised in the sand bed under the cyclic loads. The displacement fields are clearly very different for the cyclic loading compared with from the quasi-static loading. Under the ultimate load, approximately a triangular wedge of dead zone (with a constant amount of resultant displacement of the grains but has the highest vertical displacement (Fig. 3 (i)) is formed beneath the base of the footing in all cases of loadings. It is worth mentioning that the dead zone does not mean that the grains are not moving at all but move as a block of grains with almost the same magnitude of displacement [15], [16]. The depth of this wedge at the ultimate bearing load is equal to about $0.6B$, $0.8B$, and $0.7B$ for quasi-static, type1 and type2, respectively. The relatively higher value of the resultant displacement occurs in the case of footing subjected to the type 2 loading.

As seen in Fig. 3, there is considerably more horizontal spread of the displacement in the sand due to the cyclic loads

than in the quasi-static load where the vertical soil displacements tend to dominate. The 'general shear' type failure mechanism [38] is more dominant in the dense sands bed under the loading conditions considered here. The boundaries of the zone of plastic flow at failure load profiled using the advanced DPIV here are fairly similar to such intuitive diagrams suggested by Terzaghi's in 1940s [38]. In general, the vertical displacement component significantly diminished in magnitude at a depth of $z/B > 2$.

V. CONCLUSION

In this study, DPIV is used to understand the local scale geomechanical deformation characteristics of an axially loaded rigid strip footing under different types of cyclic loading and quasi-static load. The displacement patterns in the sand are studied qualitatively and quantitatively from the output of the DPIV experiments.

There is significantly more horizontal displacement in the cyclic loading types considered here than in the quasi-static loading where vertical soil displacements tend to dominate. This is due to the increase in the width of the active zones that pushed the sand grains outward and upward to the ground surface relatively more under the cyclic loading as confirmed by DPIV here. The DPIV analyses show a general shear failure mechanism in the dense sand for all types of loading considered here. Overall, the deformation behavior of sand bed is sensitive to the type of the loading considered here. Further studies are ongoing to compare the current experimental results with established numerical methodologies such as FEM, and for more types of the cyclic loading environments to get better understandings on the mechanics of sand-structure interactions in future.

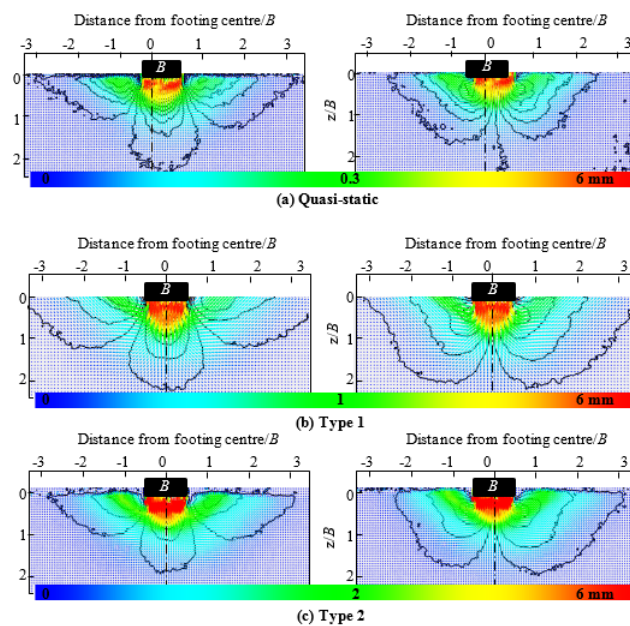


Fig. 3 Map of the mean resultant displacement vector under the ultimate load for the quasi-static and cyclic tests (i) vertical displacement (ii) horizontal displacement

ACKNOWLEDGMENT

Z. K. Jahanger acknowledges the Ministry of Higher Education and Scientific Research (MOHESR), Republic of Iraq and the University of Baghdad for the doctorate scholarship (Grant No. 2075).

REFERENCES

- [1] Das, B. M. and Shin, E. C. 1996. Laboratory model tests for cyclic load-induced settlement of a strip foundation on a clayey soil. *Geotech Geolog Eng* 14(3):213-225.
- [2] Sabbar A, Chegenizadeh A, Nikraz H (2016) Review of the experimental studies of the cyclic behaviour of granular materials: Geotechnical and pavement engineering. *Aust Geomech J* 51(2): 89-103.
- [3] Peralta P (2010) Investigations on the behavior of large diameter piles under Long-Term lateral cyclic loading in cohesionless soil. IGtH, Germany.
- [4] Shajarati A, Sørensen KW, Nielsen SK, Ibsen LB (2012) Behaviour of cohesionless soils during cyclic loading. Department of Civil Engineering, Aalborg University, Denmark.
- [5] Terzaghi K, Peck RB, Mesri G (1996) *Soil mechanics in engineering practice*. Wiley, New York.
- [6] Salem M, Elmamlouk H, Agaiby S (2013) Static and cyclic behavior of North Coast calcareous sand in Egypt. *Soil Dyn Earthq Eng* 55:83-91.
- [7] Andersen KH (2009) Bearing capacity under cyclic loading—offshore, along the coast, and on land. *Can Geotech J* 46:513-535, <https://doi.org/10.1139/T09-003> ANSYS17.2. 2017.
- [8] Raymond GP, Komos FE (1978) Repeated load testing of a model plane strain footing. *Can Geotech J* 15(2):190-201.
- [9] Tafreshi SM, Mehrjardi GT, Ahmadi M (2011) Experimental and numerical investigation on circular footing subjected to incremental cyclic loads. *Int J Civ Eng* 9(4): 265-274.
- [10] Nguyen N-S, François S, Degrande G (2014) Discrete modeling of strain accumulation in granular soils under low amplitude cyclic loading. *Comput Geotech* 62:232-243.
- [11] Asakereh A, Ghazavi M, Tafreshi SM (2013) Cyclic response of footing on geogrid-reinforced sand with void. *Soils Found* 53(3):363-374.
- [12] Jahanger ZK, Antony SJ, Richter L (2016) Displacement patterns beneath a rigid beam indenting on layered soil. In: 8th Americas Reg Conf Int Soc Terr-Veh Sys Michigan, USA.
- [13] Jahanger ZK, Antony SJ (2017a) Application of digital particle image velocimetry in the analysis of scale effects in granular soil. In: *Proceedings Pro 19th Int Conf Soil Mech Dyn.*, 9(7) part X, Rome, pp.1134-1139.
- [14] Jahanger ZK, Antony SJ (2017b) Application of particle image velocimetry in the analysis of scale effects in granular soil. *Int J Civ Enviro Stru Const Archit Eng* 11(7):832-837.
- [15] Jahanger ZK, Sujatha J, Antony SJ (2018a) Local and global granular mechanical characteristics of grain–structure interactions. *Ind Geotech J*. 10.1007/s40098-018-0295-5.
- [16] Jahanger ZK, Antony SJ, Martin E, Richter L (2018b) Interaction of a rigid beam resting on a strong granular layer overlying weak granular soil: Multi-Methodological Investigations. *J Terramech* 79:23-32.
- [17] Jahanger ZK (2018) *Micromechanical Investigations of Foundation Structures-Granular Soil Interactions*. PhD thesis, University of Leeds.
- [18] ASTM (1989) *Soil and Rock, Building, Stores, Geotextiles*. American Society for Testing and Materials, ASTM Standard. 04.08.
- [19] Head KH (2006) *Manual of Soil Laboratory Test. Volume 1: soil Classification and Compaction Tests*. CRC Press, Boca Raton, FL.
- [20] Cerato B, Lutenegeger A J (2007) Scale effects of shallow foundation bearing capacity on granular material. *J Geotech Geoenviron Eng* 133:1192-1202.
- [21] Dijkstra J, Gaudin C, White DJ, (2013) Comparison of failure modes below footings on carbonate and silica sands. *Int J Phy Model Geotech* 13(1):1-12.
- [22] Tehrani FS, Arshad MI, Prezzi M, Salgado R (2017) Physical modeling of cone penetration in layered sand. *J Geotech and Geoenviron Eng* 144(1): p04017101.
- [23] Lau CK (1988) *Scale effects in tests on footings*. PhD thesis, University of Cambridge.
- [24] Kumar J, Bhoi MK (2009) Interference of two closely spaced strip footings on sand using model tests. *J Geotech Geoenv Eng* 135(4):595-604.
- [25] Adrian RJ (1991) Particle-imaging techniques for experimental fluid mechanics. *Ann Rev Fluid Mech* 23: 261-304.
- [26] Hamm E, Tapia F, Melo F (2011) Dynamics of shear bands in a dense granular material forced by a slowly moving rigid body. *Phys Rev E*, 84: 041304.
- [27] O'Loughlin C, Lehane B (2010) Nonlinear cone penetration test-based method for predicting footing settlements on sand. *J Geotech Geoenv Eng* 136(3): 409-416.
- [28] Murthy T G, Gnanamanickam E, Chandrasekar S (2012) Deformation field in indentation of a granular ensemble. *Phys. Rev. E*, 85: 061306.
- [29] DantecDynamicsA/S (2013) *DynamicStudio User's Guide*. Dantec Dynamics, Skovlunde, Denmark.
- [30] Albaraki S, Antony, SJ (2014) How does internal angle of hoppers affect granular flow? *Experimental studies using Digital Particle Image Velocimetry*. *Powd Tech* 268:253-260.
- [31] Gollin D, Brevis W, Bowman ET, Shepley P (2017) Performance of PIV and PTV for granular flow measurements. *Granular Matter*, 19(3):42. DOI 10.1007/s10035-017-0730-9.
- [32] Vesic AS, (1973) Analysis of ultimate loads of foundations. *Soil Mech Found Div* 99(SM1): 45-73.
- [33] Das BM (2016) *Principles of foundation engineering*. 8th edition, Cengage learning, India.
- [34] Altaee A, Fellenius BH (1994) Physical modeling in sand. *Can Geotech J* 31:420-431.
- [35] Bowles JE (1996). *Foundation Analysis and Design*. Fifth ed. McGraw-Hill, Singapore.
- [36] Raymond GP (2002) Reinforced ballast behaviour subjected to repeated load. *Geotext Geomemb* 20(1):39-61.
- [37] Tafreshi SM, Dawson A (2012) A comparison of static and cyclic loading responses of foundations on geocell-reinforced sand. *Geotext Geomemb* 32:55-68.
- [38] Terzaghi, K., 1943. *Theoretical Soil Mechanics*, John Wiley and Sons Inc., New York.